LATTICE INVESTIGATIONS OF THE QCD PHASE DIAGRAM FROM ANALYTICAL CONTINUATION*

Jana N. Guenther[a,b], Szabolcs Borsányi[b], Attila Pásztor[b]
Zoltan Fodor[b,c,d], Matteo Giordano[d], Kornél Kapás[d]
Sandor D. Katz[d], Israel Portillo[e], Claudia Ratti[e], K.K. Szabó[c]

[a]University of Regensburg, Universitätsstraße 31, 93053 Regensburg, Germany
[b]University of Wuppertal, Gaußstraße 20, 42119 Wuppertal, Germany
[c]Jülich Supercomputing Centre, Forschungszentrum Jülich
52425 Jülich, Germany
[d]Institute for Theoretical Physics, Eötvös Loránd University
Pázmány Péter sétány 1/A, 1117 Budapest, Hungary
[e]Department of Physics, University of Houston, Houston, TX 77204, USA

(Received February 5, 2019)

At zero baryon density, lattice QCD is an established tool that provides precise theoretical results. Calculations at non-zero densities, however, require new techniques to deal with the sign problem. In this work, we will review our recent effort to investigate QCD at non-vanishing baryon chemical potential.

DOI:10.5506/APhysPolBSupp.12.439

1. Introduction

Correlations of conserved charges are important observables for the investigations of finite-density QCD. In this work we will summarize our results published in [1]. We will then explore the possibility to constrain the critical endpoint with these fluctuations as presented in [2]. In the following, we will use the notation $\chi^{\mathrm{B,Q,S}}_{i,j,k} = \frac{\partial^{i+j+k}(p/T^4)}{(\partial\hat{\mu}_\mathrm{B})^i(\partial\hat{\mu}_\mathrm{Q})^j(\partial\hat{\mu}_\mathrm{S})^k}$ with $\hat{\mu} = \mu/T$.

2. Fluctuations

We present results of an high-precision analysis on an $48^3 \times 12$ lattice. A more detailed description as well as precise information on the lattice set-up can be found in Refs. [1, 3]. We use analytical continuation from imaginary

* Presented at the XIII Workshop on Particle Correlations and Femtoscopy, Kraków, Poland, May 22–26, 2018.

chemical potential to determine the χ^{B} fluctuations at $\mu_{\mathrm{B}} = 0$. We analyze data for eight different values of $\mu_{\mathrm{B}} = \mathrm{i}\frac{j\pi}{8}$ with $j \in \{0, 1, 2, 3, 4, 5, 6, 7\}$. In our analysis, we use the following Ansatz for the pressure:

$$\chi_0^{\mathrm{B}}(\hat{\mu}_{\mathrm{B}}) = \frac{p}{T^4} = c_0 + c_2\hat{\mu}_{\mathrm{B}}^2 + c_4\hat{\mu}_{\mathrm{B}}^4 + c_6\hat{\mu}_{\mathrm{B}}^6 + \frac{4!}{8!}c_4\epsilon_1\hat{\mu}_{\mathrm{B}}^8 + \frac{4!}{10!}c_4\epsilon_2\hat{\mu}_{\mathrm{B}}^{10}\,, \quad (1)$$

where ϵ_1 and ϵ_2 are drawn randomly from a normal distribution with $\mu = -1.25$ and $\sigma = 2.75$. The values were chosen in a way to allow for χ_8^{B} to take the value predicted by the hadron resonance gas, as well as the result from the toy model introduced in Section 3. From the Ansatz, we can calculate the derivatives that can be measured on the lattice:

$$\chi_1^{\mathrm{B}}(\hat{\mu}_{\mathrm{B}}) = 2c_2\hat{\mu}_{\mathrm{B}} + 4c_4\hat{\mu}_{\mathrm{B}}^3 + 6c_6\hat{\mu}_{\mathrm{B}}^5 + \frac{4!}{7!}c_4\epsilon_1\hat{\mu}_{\mathrm{B}}^7 + \frac{4!}{9!}c_4\epsilon_2\hat{\mu}_{\mathrm{B}}^9\,, \quad (2)$$

$$\chi_2^{\mathrm{B}}(\hat{\mu}_{\mathrm{B}}) = 2c_2 + 12c_4\hat{\mu}_{\mathrm{B}}^2 + 30c_6\hat{\mu}_{\mathrm{B}}^4 + \frac{4!}{6!}c_4\epsilon_1\hat{\mu}_{\mathrm{B}}^6 + \frac{4!}{8!}c_4\epsilon_2\hat{\mu}_{\mathrm{B}}^8\,, \quad (3)$$

$$\chi_3^{\mathrm{B}}(\hat{\mu}_{\mathrm{B}}) = 24c_4\hat{\mu}_{\mathrm{B}} + 120c_6\hat{\mu}_{\mathrm{B}}^3 + \frac{4!}{5!}c_4\epsilon_1\hat{\mu}_{\mathrm{B}}^5 + \frac{4!}{7!}c_4\epsilon_2\hat{\mu}_{\mathrm{B}}^7\,, \quad (4)$$

$$\chi_4^{\mathrm{B}}(\hat{\mu}_{\mathrm{B}}) = 24c_4 + 360c_6\hat{\mu}_{\mathrm{B}}^2 + c_4\epsilon_1\hat{\mu}_{\mathrm{B}}^4 + \frac{4!}{6!}c_4\epsilon_2\hat{\mu}_{\mathrm{B}}^6\,. \quad (5)$$

We perform a correlated fit for $\chi_1^{\mathrm{B}}(\hat{\mu}_{\mathrm{B}})$, $\chi_2^{\mathrm{B}}(\hat{\mu}_{\mathrm{B}})$, $\chi_3^{\mathrm{B}}(\hat{\mu}_{\mathrm{B}})$ and $\chi_4^{\mathrm{B}}(\hat{\mu}_{\mathrm{B}})$ for the different values of μ_{B} to determine the fitting parameters c_2, c_4 and c_6. From the parameters, we can determine $\chi_2^{\mathrm{B}}(0) = 2c_2$, $\chi_4^{\mathrm{B}}(0) = 24c_4$, $\chi_6^{\mathrm{B}}(0) = 720c_6$ and $\chi_8^{\mathrm{B}}(0) = 24c_4\epsilon_1$. The results are shown in figure 1. These equations show the relation between χ_4^{B} and χ_8^{B} that are just related by the factor of ϵ_1 (in the same way χ_4^{B} and χ_{10}^{B} are related by a factor of ϵ_2). In this way, we take into account the influence of higher order corrections to our fit function. We choose 1000 different values for ϵ_1 and ϵ_2 and, in addition, we include either seven or eight different values of μ_{B} in our data. All resulting fits are combined in a histogram and weighted with the Akaike information criteria [4], thus alowing to estimate the systematic error. The statistical error is determined by the Jackknife method and both errors are added quadratically to get the combined error shown in the plots.

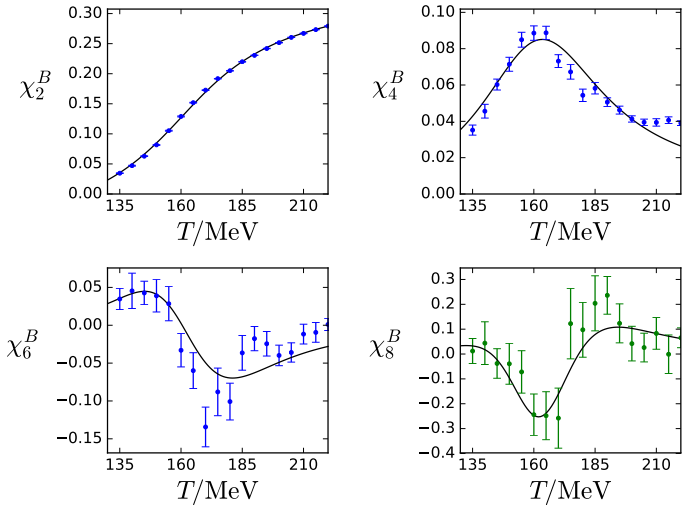

Fig. 1. (Colour on-line) Results for χ_2^{B}, χ_4^{B}, χ_6^{B} and an estimate for χ_8^{B} on a $N_t = 12$ lattice as functions of the temperature, obtained from the single-temperature analysis (see the text). We plot χ_8^{B} in green to point out that its determination is guided by a prior, which is linked to χ_4^{B}. The black curve in each panel corresponds to the toy model introduced in [1, 5].

3. Looking for the critical point

To look for the critical endpoint in the QCD phase diagram, one can try to calculate the radius of convergence of an expansion in μ_{B}. Two obvious expansions for this are either the pressure

$$p(\mu) = p_0 + p_2\hat{\mu}^2 + p_4\hat{\mu}^4 + p_6\hat{\mu}^6 + \ldots \tag{6}$$

or the fluctuations that are directly related

$$\chi_2^{\mathrm{B}}(\mu) = 2p_2 + 12p_4\hat{\mu}^2 + 30p_6\hat{\mu}^4 + \ldots \tag{7}$$

We define

$$r_{2n}^p = \sqrt{\frac{p_{2n}}{p_{2n+2}}} \qquad \text{and} \qquad r_{2n}^\chi = \sqrt{\frac{2n(2n-1)}{(2n+1)(2n+2)}} r_{2n}^p \,. \tag{8}$$

In the limit of $n \longrightarrow \infty$, both r_{2n}^p and r_{2n}^χ converge to the same value which is the radius of convergence and which guarantees that there is no criticality within this radius. However, since we only know the fluctuations up to χ_8^{B} as discussed in the previous section, we will first test this procedure for a toy

model in which the critical endpoint is known. We use unimproved staggered fermions on an $N_t = 4$ lattice. For this set up, the critical endpoint has been already determined [2, 6, 7]. The results for r^p_{2n} and r^χ_{2n} are shown in the left panel of figure 2. For a temperature where the critical endpoint is close by (right site of the left panel of figure 2), the ratios seem to converge to the correct value. However, as discussed in more detail in Ref. [2], due to the structure of χ^{B}_6, there is always a temperature for which the ratios seem to converge, independent of the real value for the critical point. For the $N_t = 12$ data, the r^χ_{2n} and the ratios from the hadron resonance gas are shown in the right panel of figure 2. Here, the errors are still large.

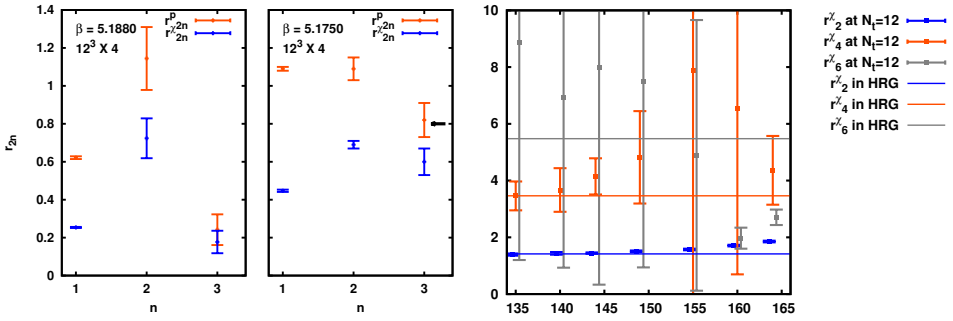

Fig. 2. On the left panel: The ratios r^p_{2n} and r^χ_{2n} (Eq. (8)) on an $N_t = 4$ lattice. On the very left, the temperature is close to the crossover temperature. Next to it, the temperature is close to the temperature for the critical endpoint. The black arrow marks the value for the critical endpoint from [7]. On the right panel: The r^χ_{2n} (Eq. (8)) ratios for different temperatures [2].

Instead of investigating a toy model with a known critical endpoint, we can also try to describe the data with a toy model without any critical behavior. If one fits the data for $\chi^{\mathrm{B}}_1/\hat{\mu}_{\mathrm{B}}$ at $\mu_{\mathrm{B}} = 0$ with an analytic function of T and assumes that any change with respect to the chemical potential is a linear shift of this function, one can determine all fluctuations analytically (more detail on this toy model can be found in Ref. [5]). The results of this toy model are shown with black curves in figure 1. They agree well with the data.

The project was funded by the DFG grant SFB/TR55. This work was supported by the Hungarian National Research, Development and Innovation Office, NKFIH grants KKP126769 and K113034. An award of computer time was provided by the INCITE program. This research used resources of the Argonne Leadership Computing Facility, which is a DOE Office of Science User Facility supported under contract DE-AC02-06CH11357. The

authors gratefully acknowledge the Gauss Centre for Supercomputing e.V. (`www.gauss-centre.eu`) for funding this project by providing computing time on the GCS Supercomputer JUQUEEN [8] at Jülich Supercomputing Centre (JSC) as well as on HAZELHEN at HLRS Stuttgart, Germany. This material is based upon work supported by the National Science Foundation under grants No. PHY-1654219 and OAC-1531814 and by the U.S. Department of Energy, Office of Science, Office of Nuclear Physics, within the framework of the Beam Energy Scan Theory (BEST) Topical Collaboration. C.R. acknowledges also the support from the Center of Advanced Computing and Data Systems at the University of Houston.

REFERENCES

[1] S. Borsanyi *et al.*, *J. High Energy Phys.* **1810**, 205 (2018) [`arXiv:1805.04445 [hep-lat]`].

[2] Z. Fodor *et al.*, Searching for a CEP Signal with Lattice QCD Simulations, in: Proc. of 27$^{\text{th}}$ International Conference on Ultrarelativistic Nucleus–Nucleus Collisions (Quark Matter 2018), Venice, Italy, May 14–19, 2018.

[3] R. Bellwied *et al.*, *Phys. Rev. D* **92**, 114505 (2015).

[4] H. Akaike, *IEEE Trans. Automat. Contr.* **19**, 716 (1974).

[5] S. Borsanyi *et al.*, Towards the Equation of State at Finite Density from the Lattice, in: Proc. of 27$^{\text{th}}$ International Conference on Ultrarelativistic Nucleus–Nucleus Collisions (Quark Matter 2018), Venice, Italy, May 14–19, 2018.

[6] Z. Fodor, S.D. Katz, *J. High Energy Phys.* **0203**, 014 (2002).

[7] Z. Fodor, S.D. Katz, *J. High Energy Phys.* **0404**, 050 (2004).

[8] Jülich Supercomputing Centre, *Journal of large-scale research facilities* **A1**, 1 (2015).